Journal of Hazardous Materials 174 (2010) 175–180

Contents lists available at ScienceDirect

Journal of Hazardous Materials

journal homepage: www.elsevier.com/locate/jhazmat

A molecular dynamics simulation of solvent effects on the crystal morphology of HMX

Xiaohui Duan[a,b,*], Chunxue Wei[a], Yonggang Liu[c], Chonghua Pei[a]

[a] College of Materials Science and Engineering, Southwest University of Science and Technology, Mianyang 621010, China
[b] Institute of Fluid Physics, China Academy of Engineering Physics, Mianyang 621900, China
[c] Institute of Chemical Materials, China Academy of Engineering Physics, Mianyang 621900, China

ARTICLE INFO

Article history:
Received 13 July 2009
Received in revised form 5 September 2009
Accepted 7 September 2009
Available online 15 September 2009

Keywords:
Crystal morphology
HMX
AE model
Molecular dynamics simulation

ABSTRACT

The solvent has a large effect on the crystal morphology of the organic explosive compound octahydro-1,3,5,7-tetranitro-1,3,5,7-tetrazocine (HMX, $C_4H_8N_8O_8$). The attachment energy calculations predict a growth morphology in vacuum dominated by (0 2 0), (0 1 1), (1 0 $\bar{2}$), (1 1 $\bar{1}$) and (1 0 0) crystal forms. Molecular dynamics simulations are performed for these crystal faces of HMX in contact with acetone solvent. A corrected attachment energy model, accounting for the surface chemistry and the associated topography (step structure) of the habit crystal plane, is applied to predict the morphological importance of a crystal surface in solvent. From the solvent-effected attachment energy calculations it follows that the (1 0 0) face becomes morphologically more important compared with that in vacuum, while the (0 2 0) and (1 0 $\bar{2}$) are not visible at all. This agrees well with the observed experimental HMX morphology grown from the acetone solution.

1. Introduction

The control of crystal morphology during the crystallization steps constitutes an important industrial challenge since the shape of a crystal affects solid–liquid separation characteristics, packaging, handling, drying, storage behavior and end-use properties of the crystallized material. For the explosive compounds, an important product performance parameter is the packing density. A high packing density is needed to obtain a high explosive power in a small volume. The particle shape largely determines the packing density. Needles and plate-like crystal have a low density and thus are unwanted shapes. Higher packing densities can be obtained with isometric crystals. Besides, the sensitivity of the explosive compound is dependent on the crystal morphology to a great extent. Therefore, investigations on crystal morphology control are very important for the energetic materials.

The morphology of a growing crystal is governed by two factors, the internal structure of a crystal and external parameters, such as supersaturation, temperature level, the presence of solvents and impurities. Among them, solvent is one of the most important factors that should be taken into account. The determination of the basic crystal morphology, as well as the assessment of the solvent effects on the crystal morphology, becomes more and more important in modern industry. A great number of attempts have been made to investigate the solvent effects on the crystal morphology experimentally and theoretically (simulation) [1–15]. In this, the work of Lahav and Leiserowitz [1,2] is seminal in relating the mechanistic aspects associated with habit modification to the specificity of the intermolecular interactions between crystallographically ordered crystal habit surfaces and solvent/or impurity molecules. In a later review article [3], the influence of the solvent environment on the crystal morphology for a number of amino acids was reviewed. Enthalpy changes associated with the docking of solvent molecules on specific crystal surfaces have been used to predict the morphology. Winn and Doherty [4] provided an excellent review of current and emerging modeling approaches in terms of practical applicability, from the standpoint of process engineering. Wang et al. [5] summarized the advances and future directions in morphology monitoring and control of organic crystal grown from solution. They pointed out that the integration of on-line real-time 3D shape measurement, multi-scale modeling of morphology, multi-dimensional population balance modeling and computational fluid dynamics is the goal of the further research. Molecular dynamics [8,9,12,13] and Monte Carlo [9–11,14,15] methods have been applied to study the most favored interactions between the crystal habit surfaces and specific solvents in order to establish the modification to the crystal shape in terms of relative growth rates.

HMX is an important and commonly used energetic ingredient in various high performance explosives and propellant formulation due to its thermal stability and high detonation velocity relative to

* Corresponding author at: College of Materials Science and Engineering, Southwest University of Science and Technology, Mianyang 621010, China.
Tel.: +86 816 2419280.
E-mail addresses: dxhui812@163.com, duanxiaohui@swust.edu.cn (X. Duan).

0304-3894/$ – see front matter © 2009 Elsevier B.V. All rights reserved.
doi:10.1016/j.jhazmat.2009.09.033

other explosives [16,17]. It is known to occur in three polymorphic forms α, β, and δ (γ-HMX identified as a hydrate) [18–20]. The industrially preferred form β-HMX is the stable form at room temperature and atmospheric pressure. Thomas et al. [21,22] have calculated the geometrical structures and mechanical properties of the three pure polymorphic forms of crystalline HMX using Monte Carlo method. ter Horst et al. [23] have determined the morphologically important surfaces of β-HMX and α-HMX with the aid of a periodic bond chain (PBC) analysis, but few examples including solvent effects on the HMX crystal morphology can be quoted. In this paper, the morphology modification of the model compound β-HMX induced by solvent is studied using the corrected attachment energy (AE) model. For the sake of convenience, we use HMX as a substitute for β-HMX in the next sections.

2. Computational details and theory

2.1. Computational details

According to neutron diffraction experiments of HMX [19], the unit cell model is constructed. Molecular mechanics potential-energy minimization is performed on the unit cell (Smart minimizer, optimization of the cell parameters). The AE model is used to predict the crystal morphology in vacuum, which gives a list of possible crystal faces with different inherent multiplicities. The morphologically important surfaces ($h\,k\,l$) can be obtained from the AE calculations. The HMX crystal is cleaved parallel to the ($h\,k\,l$) plane with a depth of four unit cell. A crystal slice is constructed as a periodic superstructure of 3×3 unit cells. Subsequently, the crystal slice is optimized by the molecular mechanics and molecular dynamics (MD) methods in turn. The chosen solvent is acetone with the reflective index n of 1.3588, static dielectric constant ε_0 of 21 and density of 0.78 g/cm^3 [24]. A solvent layer containing 200 acetone molecules is constructed by the Amorphous Cell tool and refined by MD technique. Two-layer interfacial model is employed for the MD simulation to study the influence of the solvent on the crystal shape. One part of the model is the crystal slice and another is occupied by the solvent layer, i.e., the solvent layer is adsorbed on the ($h\,k\,l$) crystal face along c axis. 50 Å thickness vacuum slab is built in above the solvent layer to eliminate the effect of additional free boundaries on the structure. The final simulation model consists of 72 HMX molecules and 200 acetone molecules (4016 atoms in total). The crystal slice is constrained during the MD simulation process. The energy minimization for the interfacial model is carried out before the dynamics simulation. MD simulation is carried out in the NVT ensemble at the HMX crystallization temperature of 550 K. The temperature control method is set to be Andersen, which chooses atom collision times from a Poisson distribution at each time step and changes their velocities according to the Boltzmann distribution [25]. For the equilibration stage, the time step for the MD simulation is 1 fs with a period of 60 ps. When equilibration has been achieved, energy and temperature fluctuate around their averages, which remain constant over time. After equilibrating the system at the target temperature, the production stage has been performed, during which data and statistics are collected. The time step is 1 fs with a period of 80 ps. All the calculations are run with the commercial molecular modeling software package Materials Studio 3.0 [26], using the Compass force field [27]. Compass is a powerful ab initio force field supporting atomistic simulations of condensed-phase materials and stands for condensed-phase optimized molecular potentials for atomistic simulation studies. For potential-energy calculations, the Coulombic and van der Waals interactions are calculated by employing the standard Ewald method [28].

2.2. Theory

The solvent can be assumed to reduce the growth rate. First, the solvent has to be removed from the surface before the crystal face can grow. This costs energy and herewith the apparent attachment energy decreases. An energy correction term E_s for the vacuum attachment energy E_{att} can be introduced which represents this solvent effect

$$E_{att}^s = E_{att} - E_s \tag{1}$$

where E_{att}^s denotes the solvent-effected attached energy. A crystal surface becomes morphologically more important if, due to specific solvent interactions with this crystal surface, the attachment energy of a ($h\,k\,l$) slice is decreased more than the attachment energies of the other ($h\,k\,l$) slices. The calculations of all the surface specific energy correction terms E_s ($h\,k\,l$) then result in a solvent influenced morphology prediction.

Since the effect of solvent depends on both the different surface chemistry and the associated topography (step structures) of the crystal face, the correction term E_s describing the energy of solvent binding on the crystal habit surface ($h\,k\,l$) can be calculated using the following formula:

$$E_s = \frac{E_{\text{int}} A_{\text{acc}}}{A_{\text{model}}} \tag{2}$$

where E_{int} is the interaction energy between the solvent layer and the surface, A_{model} is the surface area of the simulated model in the ($h\,k\,l$) direction, and A_{acc} is the accessible solvent surface of the crystal face in the unit cell. E_{int} is evaluated using the relationship:

$$E_{\text{int}} = E_{\text{tot}} - E_{\text{surf}} - E_{\text{solv}} \tag{3}$$

where E_{tot} is the total energy of the surface and the solvent layer, E_{surf} is the energy of the surface without the solvent layer, and E_{solv} is the energy of the solvent layer without the surface. Binding energy is defined as the negative value of the interaction energy, that is,

$$E_b = -E_{\text{int}} \tag{4}$$

The accessible solvent surface A_{acc} is obtained by calculating the Connolly surface. The Connolly surface [29] modeling, i.e., which revealed the van der Waals surface of the host system accessible to the solvent molecules, is used to provide a quantitative approach for locating the regions of the crystal surface, which would be likely areas for solvent binding.

The relative growth rate for each face is taken to be proportional to E_{att}^s [see formula (5)] [30,31], and hence face with the lowest attachment energy is predicted to be the slowest growing surface and hence to have the highest morphological importance.

$$R \propto E_{att}^s \tag{5}$$

3. Re-crystallization experiment

The raw HMX material is provided by Institute of Chemical Materials, China Academy of Engineering Physics. The temperature dependence of the HMX solubility in the acetone solvent is used to determine the supersaturation. 0.75 g HMX is dissolved in 25 mL acetone solvent (analytical grade) under agitation and then slowly heated up to 60 °C on a water bath maintained at constant temperature to make it completely dissolved. The resulting solution is cooled down to ambient temperature. Seed crystals are obtained by spontaneous nucleation when the acetone solvent is gradually evaporated. The morphology of the final HMX crystal is observed using the SEM (TM-1000, Hitachi, Japan).

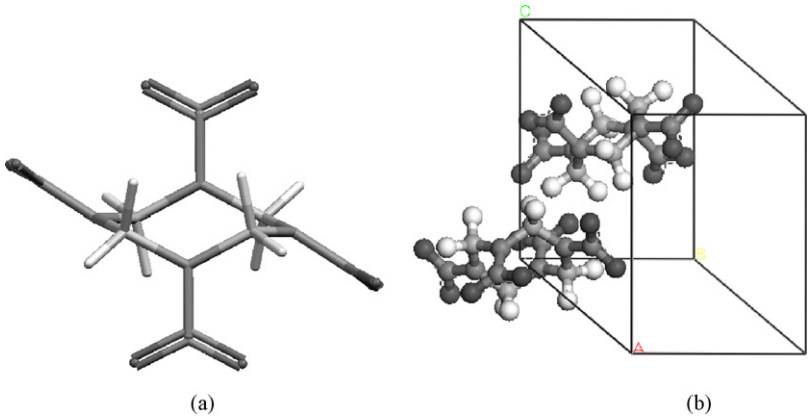

Fig. 1. Molecular (a) and crystal (b) structures of HMX.

4. Results and discussions

HMX molecular conformation in HMX unit cell is depicted in Fig. 1(a). HMX crystal belongs to the monoclinic system (a = 6.54 Å, b = 11.05 Å, c = 8.70 Å, β = 124.31°, R = 5.9%, ρ = 1.8937 g/cm^3) with $P2_1/c$ symmetry and 2 molecules per unit cell (see Fig. 1(b)) [19]. The external morphology of crystals is predicted using the AE model based on the optimized unit cell geometry. The morphology in vacuum is displayed in Fig. 2(a). The prediction of the crystal shape according to the AE model results in a shape similar to the hexahedron with an aspect ratio of 2.06. The unique exhibiting faces are (0 2 0), (0 1 1), (1 0 $\bar{2}$), (1 1 $\bar{1}$) and (1 0 0). The (0 1 1) face is morphologically the most important whose percentage area is above 60%. Its E_{att} is calculated to be 26.01 kcal/mol comprised of the electrostatic interaction (12.26 kcal/mol) and van der Waals force (13.75 kcal/mol). The (1 1 $\bar{1}$) face has 29.9% area to be the second large existing surface. The (1 0 0) and (1 0 $\bar{2}$) faces have almost equal existing area, 1.76% and 1.61%, respectively.

The crystal packing diagrams (see Fig. 2) reveal the surface chemistry and topography of the HMX crystal habit faces. Examination of the (1 0 0) face reveals a rather open and rough surface topography on the molecular level with the nitro groups of the HMX molecules exposed out of the surface. The (0 1 1), (1 1 $\bar{1}$) and (0 2 0) habit faces are found to be smooth on the molecular level. Both oxygen and hydrogen atoms are observed to be exposed at the (0 1 1) and (1 1 $\bar{1}$) surfaces, different only from the densities and positions. With respect to the (0 2 0) surface, the surface chemistry is mainly dominated by the exposed oxygen atoms. The (1 0 $\bar{2}$) face is found to be very smooth on the molecular level allowing the exposure of only the hydrogen atoms of the HMX molecules.

Table 1
Surface areas for the crystal habit surfaces.

Surface	(0 1 1)	(1 1 $\bar{1}$)	(0 2 0)	(1 0 0)	(1 0 $\bar{2}$)
A_{acc} (Å^2)	112.560	143.902	73.899	197.793	139.432
A_{hkl}[a] (Å^2)	86.208	94.041	47.003	96.135	120.299
S[b]	1.306	1.530	1.572	2.057	1.159

[a] The surface area of the crystal face ($h\,k\,l$) in unit cell.
[b] The accessible solvent surface of unit area.

The results for the surface area of the crystal face are presented in Table 1. For the Connolly surface calculations, the grid interval is 0.4000 Å at a probe radius of 1.0 Å. The accessible solvent surface of unit crystal area denoted as S in Table 1 is calculated convenient for comparing the step structures of different crystal faces. From Table 1, we can find that the (1 0 0) face has the highest S value, while the (1 0 $\bar{2}$) has the least S value among all the exhibiting surfaces. The A_{acc} and S calculations quantitatively indicate the difference of the step structures of the crystal faces. The HMX–acetone solvent interfaces for five different crystal faces are shown in Fig. 3, which illustrates the affinity ability of the acetone solvent on the particular crystal face. The interaction energies of the solvent molecules on the different habit faces are listed in Table 2, column 5. The interaction energy calculations and the snapshots of the solute/solvent interfaces indicate the different degrees of solvent binding on the habit faces. For the (1 0 0) surface, the interfacial snapshot indicates that the solvent molecules have moved into the crystal face and formed a dense solvent layer. This should owe to the face-specific and much strong solvent–solute interaction of −177.28 kcal/mol. We analyze the result looking at the

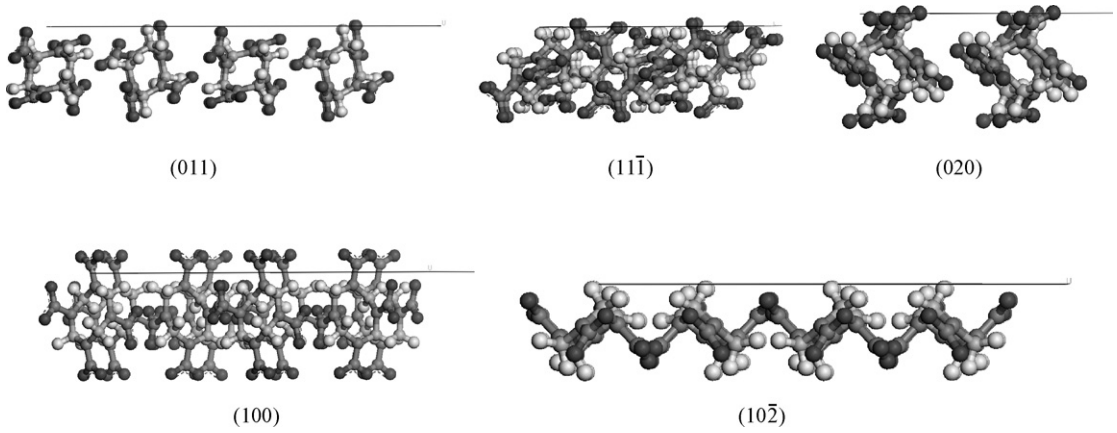

Fig. 2. Molecular arrangement of the crystal face of HMX, 2 × 2 supercell.

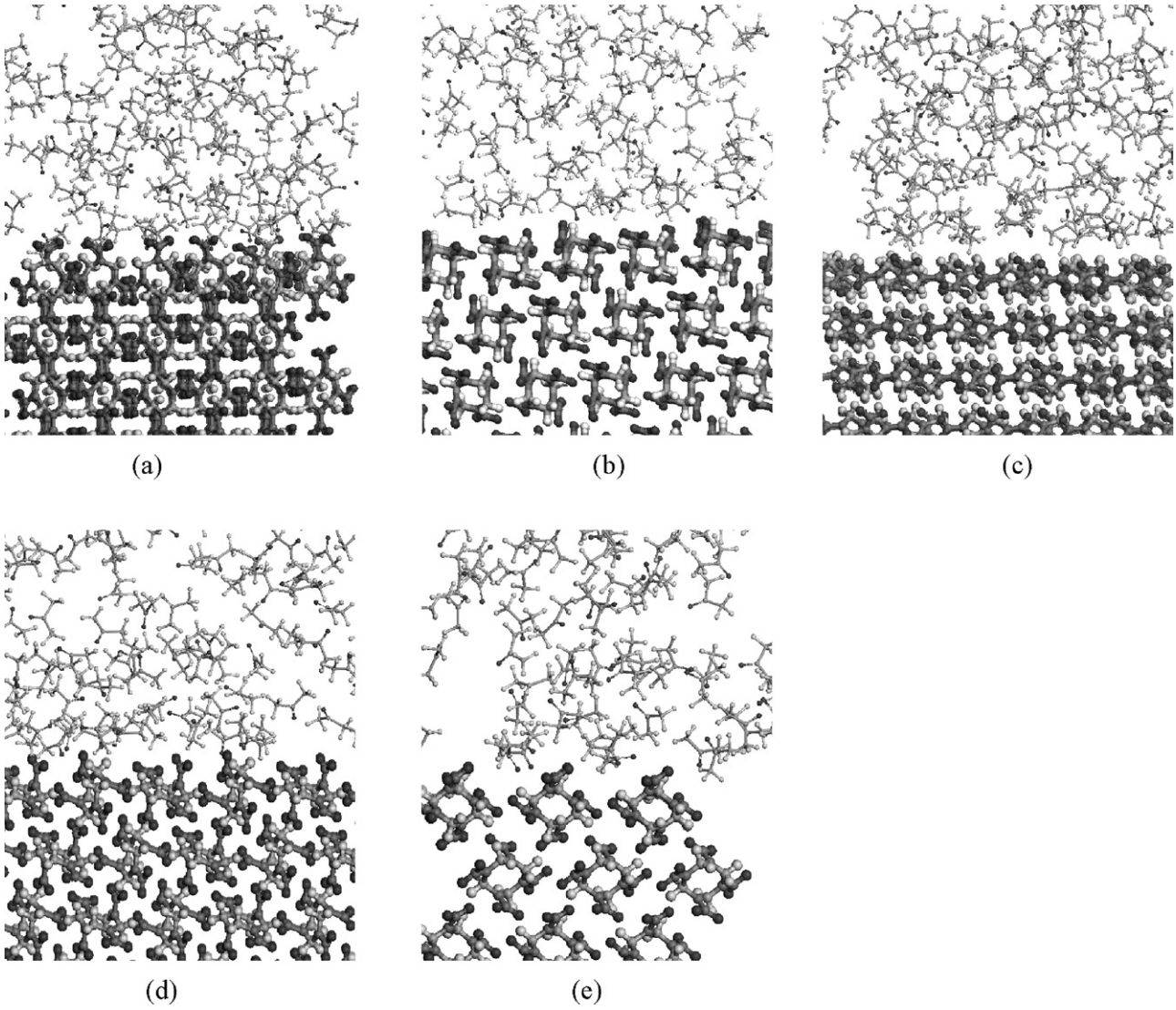

Fig. 3. Snapshots from the molecular dynamics simulations of the HMX–acetone solvent interfaces. (a), (b), (c), (d) and (e) correspond to (1 0 0), (0 1 1), (1 0 $\bar{2}$), (1 1 $\bar{1}$) and (0 2 0) crystal faces, respectively.

three contributions present in the compass force field: the van der Waals energy, the Coulomb energy, and the hydrogen-bond energy. The three contributions to the energy as well as the total energy are averaged for the MD run. The solvent binding energy of 177.28 kcal/mol for the (1 0 0) surface is principally caused by the van der Waals energy (103.94 kcal/mol), followed by the Coulomb contribution (73.34 kcal/mol), without hydrogen-bond interaction. Contrary to the (1 0 0) surface, the (0 2 0) face has the lowest binding energy of 80.08 kcal/mol, also comprised of van der Waals energy (58.63 kcal/mol) and Coulomb energy (21.45 kcal/mol).

Table 2 and Fig. 4 summarize the results from these simulations and experimentally observed crystal habits for HMX growth from the acetone solution. It can be found that the relative growth rates of the (0 1 1) and (1 1 $\bar{1}$) faces have negligible change in acetone solution; solvent effects have brought out of significant change of the growth rates for other faces. Accordingly, the crystal habit is largely different from that in vacuum. A comparison of Fig. 4(a) and (b) reveals that the (0 2 0) and (1 0 $\bar{2}$) disappear due to the faster growth, while the (1 0 0) face becomes the morphologically important crystal face for the growth retardation in the presence

Table 2
Calculated attachment energies for dominant crystal habit faces together with corrected attachment energies and relative growth rates of faces[a].

Face	d_{hkl}[b]	E_{att}	R[c]	E_{int}	A_{acc}	A_{model}	E_s	E^s_{att}	R^*[d]
(0 1 1)	6.025	−26.01	1	−102.52	112.56	748.75	−15.42	−10.59	1
(1 1 $\bar{1}$)	5.523	−39.52	1.52	−138.74	143.90	838.14	−23.82	−15.70	1.48
(0 2 0)	5.525	−37.06	1.42	−80.08	73.90	444.64	−13.28	−23.78	2.24
(1 0 0)	5.403	−51.59	1.98	−177.28	197.79	834.45	−42.07	−9.52	0.90
(1 0 $\bar{2}$)	4.317	−42.28	1.62	−137.53	139.43	1019.22	−18.83	−23.45	2.21

[a] All energies are in kcal/mol, distance in Å, and area in Å^2.
[b] Lattice-plane spacing.
[c] Relative growth rate in vacuum.
[d] Relative growth rate in acetone solution.

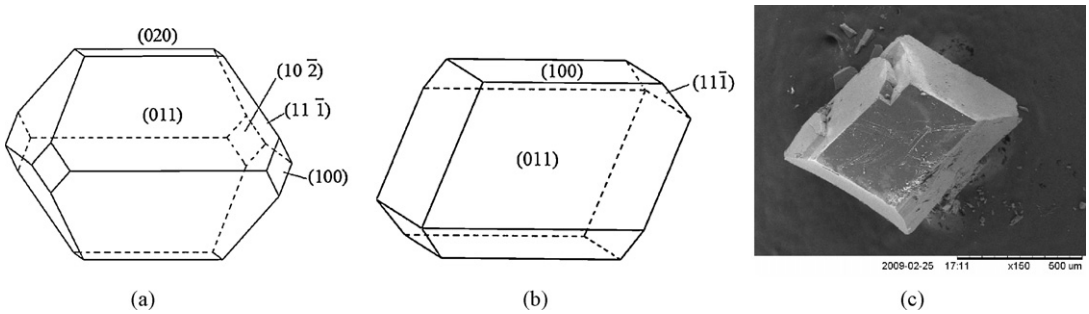

Fig. 4. Crystal habit for HMX as predicted via the AE model in vacuum (a), as derived from the corrected AE model in acetone (b), and the SEM micrograph illustrating the crystal habit re-crystallized from the acetone solution (c).

of acetone. Its percentage area increases up to 27% from the 1.76% in vacuum. The crystal habit prediction, as adjusted to allow for the solvent effects (Fig. 4(b)), provides a good match to the experimental morphology (Fig. 4(c)). As discussed above, the solvent effects depend on the different surface chemistry and the step structure of the crystal faces, and are quantified as the energy correction term E_s in our work. For example, the low growth rate of the (1 0 0) face in the acetone solvent can be attributed to the polar nitro groups exposed out of the face and large accessible solvent surface, which would be expected to be conducive to easy solvent binding. Its E_s absolute value is calculated up to 42.07 kcal/mol. So, the desolvation process becomes very difficult owing to the high energy barrier, and the solute molecules are hampered in reaching the surface. For the (0 2 0) face, in contrast, its absolute value of the E_s term has been the lowest, resulting in the fastest growth in this direction. Inspite of the nearly equal interaction energies of the (1 1 $\bar{1}$) and (1 0 $\bar{2}$) faces with the acetone molecules, the difference in the accessible solvent surface of unit area (see the *S* value in Table 1) has brought faster growth of (1 0 $\bar{2}$) face than (1 1 $\bar{1}$).

5. Conclusion

In this work, through the molecular dynamics simulations of a solvent layer of acetone adsorbed on the HMX habit crystal surface, we report the solvent-mediated crystal habit for HMX by a corrected AE model. This model takes the solvent effects on the crystal morphology as a corrected term for the attachment energy in vacuum, considering the surface chemistry and the step structure of the habit crystal plane. The crystal shape of HMX in vacuum is dominated by (0 2 0), (0 1 1), (1 0 $\bar{2}$), (1 1 $\bar{1}$) and (1 0 0) crystal faces predicted applying the AE model. The corrected attachment energy calculations suggest that the (0 2 0) and (1 0 $\bar{2}$) crystal faces will not be visible on a HMX crystal grown from the acetone solution, while the (1 0 0) face becomes morphologically more important as compared to that in vacuum. This result of the morphological prediction is in reasonable agreement with the experimental habit re-crystallized from the acetone solution. Clearly, further work is needed to test the applicability of this corrected AE model via validated studies using a number of different HMX/solvent systems and to further obtain the solvent selectivity on the crystal morphology during the solution crystallization process of HMX.

Acknowledgment

This work is supported by the National “973” Project.

References

[1] L. Addadi, Z. Berkovitch-Yellin, I. Weissbuch, M. Lahav, L. Leiserowitz, The use of “Enantiopolar” directions in centrosymmetric crystals for direct assignment of absolute configuration of chiral molecules: application to the system serine/threonine, J. Am. Chem. Soc. 104 (1982) 2075–2077.
[2] I. Weissbuch, L. Addadi, Z. Berkovitch-Yellin, E. Gati, S. Weinstein, M. Lahav, L. Leiserowitz, Centrosymmetric crystals for the direct assignment of the absolute configuration of chiral molecules. Application to the alpha-amino acids by their effect on glycine crystals, J. Am. Chem. Soc. 105 (1983) 6615–6621.
[3] M. Lahav, Z. Berkovitch-Yellin, The effect of solvent on crystal growth and morphology, Chem. Eng. Sci. 56 (2001) 2245–2253.
[4] D. Winn, M.F. Doherty, Modeling crystal shapes of organic materials grown from solution, AIChE J. 7 (2000) 1348–1367.
[5] X.Z. Wang, K.J. Roberts, J. Calderon De Anda, Advances and future directions in morphology monitoring and control of organic crystal grown from solution, in: 16th European Symposium on Computer Aided Process Engineering and 9th International Symposium on Process Systems Engineering, 2006, pp. 1611–1616.
[6] R.B. Hammond, K. Pencheva, V. Ramachandran, K.J. Roberts, Application of grid-based molecular methods for modeling solvent-dependent crystal growth morphology: aspirin crystallized from aqueous ethanolic solution, Cryst. Growth Des. 7 (2007) 1571–1574.
[7] J.X. Chen, J.K. Wang, Y. Zhang, H. Wu, W. Chen, Z.C. Guo, Crystal growth, structure and morphology of hydrocortisone methanol solvate, J. Cryst. Growth 265 (2004) 266–273.
[8] R.B. Hammond, K. Pencheva, K. Roberts, A structural-kinetic approach to model face-specific solution/crystal surface energy associated with the crystallization of acetyl salicylic acid from supersaturated aqueous/ethanol solution, Cryst. Growth Des. 6 (2006) 1324–1334.
[9] S. Piana, J.D. Gale, Understanding the barriers to crystal growth: dynamical simulation of the dissolution and growth of urea from aqueous solution, J. Am. Chem. Soc. 127 (2005) 1975–1982.
[10] S. Piana, M. Reyhani, J.D. Gale, Simulating micrometer-scale crystal growth from solution, Nature 438 (2005) 70–73.
[11] S. Piana, J.D. Gale, Three-dimensional kinetic Monte Carlo simulation of crystal growth from solution, J. Cryst. Growth 294 (2006) 46–52.
[12] C. Stoica, P. Verwer, H. Beekes, P.J.C.M. van Hoof, F.M. Kaspersen, E. Vlieg, Understanding the effect of a solvent on the crystal habit, Cryst. Growth Des. 4 (2004) 765–768.
[13] C.L. Li, P. Choi, Molecular dynamics study on the effect of solvent adsorption on the morphology of glycothermally produced α-Al_2O_3 particles, J. Phys. Chem. C 112 (2008) 10145–10152.
[14] M.A. Deij, J. van Eupen, H. Meekes, P. Verwer, P. Bennema, E. Vlieg, Experimental and computational morphology of three polymorphs of the free base of Venlafaxine: a comparison of morphology prediction methods, Int. J. Pharm. 353 (2008) 113–123.
[15] J. Kundin, C. Yürüdü, J. Ulrich, H. Emmerich, A phase-field/Monte-Carlo model describing organic crystal growth from solution, Eur. Phys. J. B 70 (2009) 403–412.
[16] P.W. Cooper, S.R. Kurowski, Introduction to the Technology of Explosives, Wiley, New York, 1996.
[17] J. Akhaven, The Chemistry of Explosives, Royal Society of Chemistry, Cambridge, UK, 1998.
[18] H.H. Cady, A.C. Larson, D.T. Cromer, The crystal structure of α-HMX and refinement of the structure of β-HMX, Acta Cryst. 16 (1963) 617–623.
[19] C.S. Choi, H.P. Boutin, A study of the crystal structure of β-cyclotetramethene tetranitramine by neutron diffraction, Acta Cryst. B26 (1970) 1235–1240.
[20] R.E. Cobbledick, R.W.H. Small, The crystal structure of the δ-form of 1,3,5,7-tetranitro-1,3,5,7-tetraazacyclooctane (δ-HMX), Acta Cryst. B30 (1974) 1918–1922.
[21] D.S. Thomas, Monte Carlo calculations of the hydrostatic compression of hexahydro-1,3,5-trinitro-1,3,5-triaine and octahydro-1,3,5,7-tetranitro-1,3,5,7-tetrazocine, J. Appl. Phys. 83 (1998) 4142–4145.
[22] P.L. James, D.S. Thomas, B.E. Richard, A.V. Gregory, Electronic structure calculation of the structures and energies of the three pure polymorphic forms of crystalline HMX, J. Phys. Chem. B104 (2000) 1009–1013.
[23] J.H. ter Horst, H.J.M. Kramer, G.M. van Rosmalen, P.J. Jansens, Molecular modeling of the crystallization of polymorphs. Part I. The morphology of HMX polymorphs, J. Cryst. Growth 237–239 (2002) 2215–2220.
[24] J.A. Dean (Ed.), Lange’s Handbook of Chemistry, 15th ed., McGraw-Hill, New York, 1999.

[25] H.C. Andersen, Molecular dynamics simulations at constant pressure and/or temperature, J. Chem. Phys. 72 (1980) 2374–2383.
[26] Materials Studio 3.0, Accelrys Inc., San Diego, CA, 2004.
[27] H. Sun, COMPASS: an ab initio force-field optimized for condensed-phase applications—overview with details on alkane and benzene compounds, J. Phys. Chem. B 102 (1998) 7338–7364.
[28] P.P. Ewald, Evaluation of optical and electrostatic lattice potentials, Ann. Phys. 64 (1921) 253–287.
[29] M.L. Connolly, Solve-accessible surfaces of proteins and nucleic acids, Science 221 (1983) 709–713;
M.L. Connolly, Analytical molecular surface calculation, J. Appl. Cryst. 16 (1983) 548–558.
[30] Z. Berkovitch-Yellin, Toward an ab initio derivation of crystal morphology, J. Am. Chem. Soc. 107 (1985) 8239–8253.
[31] P. Hartman, P. Bennema, The attachment energy as a habit controlling factor, J. Cryst. Growth 49 (1980) 145–156.